

HOW DOES A VIRTUAL AGENT DECIDE WHERE TO LOOK? - SYMBOLIC COGNITIVE REASONING FOR EMBODIED HEAD ROTATION

Juyeong Hwang^{1,*}

Seong-Eun Hong^{1,*}

JaeYoung Seon²

Hyeongyeop Kang^{1,†}

¹Korea University

²Kyung Hee University
Korea, Republic

{05judy02, seong_eun, siamiz_hkang}@korea.ac.kr
cogongnam@khu.ac.kr

August 13, 2025

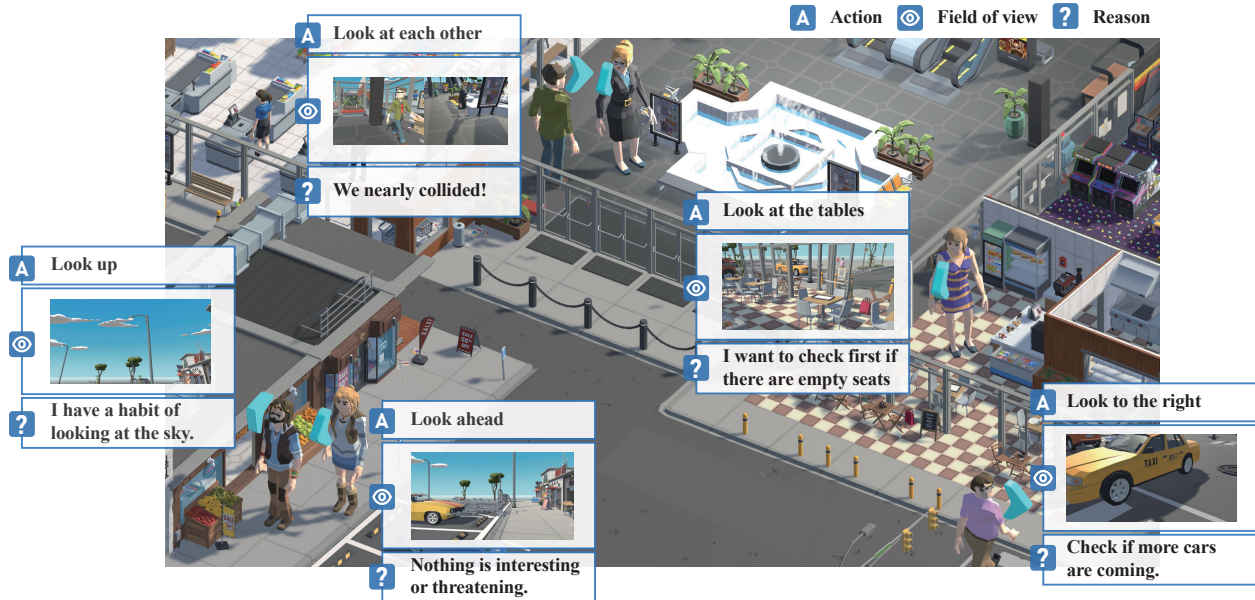


Figure 1: This example illustrates how *SCORE* produces human-like head movements in a multi-agent setting. The highlighted agent attends to the intended walking path, aligning closely with the ground-truth behavior. In contrast, *Track* fixates excessively on static background elements (e.g., storefronts), failing to handle multiple factors (e.g., secure path, understand pedestrian flow) and resulting in implausible head rotations.

*These authors contributed equally to this work.

†Corresponding author.

ABSTRACT

Natural head rotation is critical for believable embodied virtual agents, yet this micro-level behavior remains largely underexplored. While head-rotation prediction algorithms could, in principle, reproduce this behavior, they typically focus on visually salient stimuli and overlook the cognitive motives that guide head rotation. This yields agents that look at conspicuous objects while overlooking obstacles or task-relevant cues, diminishing realism in a virtual environment. We introduce **SCORE**, a **S**ymbolic **C**Ognitive **R**easoning framework for **E**mbodied Head Rotation, a data-agnostic framework that produces context-aware head movements without task-specific training or hand-tuned heuristics. A controlled VR study ($N=20$) identifies five motivational drivers of human head movements: *Interest*, *Information Seeking*, *Safety*, *Social Schema*, and *Habit*. SCORE encodes these drivers as symbolic predicates, perceives the scene with a Vision–Language Model (VLM), and plans head poses with a Large Language Model (LLM). The framework employs a hybrid workflow: the VLM-LLM reasoning is executed offline, after which a lightweight FastVLM performs online validation to suppress hallucinations while maintaining responsiveness to scene dynamics. The result is an agent that predicts not only *where* to look but also *why*, generalizing to unseen scenes and multi-agent crowds while retaining behavioral plausibility.

1 Introduction

Realistic and context-aware virtual agents have long been a central research focus in computer graphics [1, 2, 3, 4]. One of the key aspects of believable agent behavior lies in natural head rotations that reveal what it notices, what it intends, and how it handles risk.

Synthesizing such micro-behavior is a long-standing challenge. Yet recent head movement synthesizers still treat attention as a colored blob on the image plane. Trained on saliency maps [5, 6, 7, 8], they steer the camera toward the conspicuous elements while ignoring why a human might look elsewhere. Real pedestrians, for example, repeatedly scan the flow of oncoming cars, bicycles, and walkers, balancing safety, curiosity, and social convention in a single sweep. Saliency-only models over-predict attraction to bright or moving objects and under-predict purposeful reorientations guided by cognitive processes, degrading realism in cluttered, dynamic scenes.

To address these limitations, we propose *SCORE*, a **S**ymbolic **C**Ognitive **R**easoning framework for **E**mbodied head rotation. A VR study with twenty participants across ten scenarios identified five motivational drivers of human head movements: *Interest*, *Information-seeking*, *Safety*, *Social schema*, and *Habit*. *SCORE* exploits these drivers as symbolic predicates and embeds them in a two-stage controller.

An offline Deliberative Perception–Planning Stage (DPS) combines a Vision–Language Model (VLM) and a Large Language Model (LLM) to draft a time-stamped head-orientation plan. At run time, a lightweight Reactive Execution Stage (RES) validates each pose about two seconds before display with FastVLM; if the live view deviates, RES substitutes a context-appropriate alternative. In practice, this “near-online” correction rejects actions based on hallucinations, absorbs late scene edits, and lets agents respond plausibly to user maneuvers or unforeseen obstacles—all without rerunning the costly VLM–LLM loop.

In summary, our contributions are as follows:

- **Cognitive Reasoning for plausible head-motion:** We introduce *SCORE*, the first framework that synthesizes context-aware head orientations via cognitive reasoning.
- **Zero-shot generalization:** *SCORE* transfers to unseen environments without additional data, tuning, or code changes.
- **Human-inspired symbolic model:** Five motivational drivers, extracted from a VR user study, are encoded as predicates that significantly improve behavioural plausibility.
- **Hybrid control:** A semi-reactive pipeline pairs offline VLM–LLM planning with lightweight FastVLM validation, reducing hallucinations while maintaining responsiveness to scene dynamics.

2 RELATED WORK

2.1 Head-Movement Prediction

Head orientation is widely regarded as a reliable proxy for observable visual attention: in social activity or outdoor tasks, where a person turns their head often signals what they are thinking about and concentrating on [9, 10, 11, 12]. In

other words, predicting those turns requires more than stimulus detection; it calls for an understanding of the underlying cognitive intent.

Head movement prediction has been widely researched to optimize user experience in 360-degree video consumption [13, 14]. Early methods extrapolated head trajectories via linear filters [15, 16], but they ignored the link between attention and changing content. Subsequent work fused saliency with motion history; PanoSalNet + LSTM captured the equatorial bias of HMD viewers and improved accuracy during rapid turns [12]. TRACK advanced this line by balancing trajectory and saliency cues with a Structural-RNN [17], achieving state-of-the-art robustness across exploratory and focus-driven clips [8].

Despite these gains, saliency- and trajectory-based predictors remain stimulus-bound; they overlook the cognitive drivers—information seeking, habitual scanning—that govern human re-orientation. [4] argue that physically plausible motion is tied to higher-level reasoning. Our work follows this direction, using symbolic cognitive predicates and vision–language reasoning to predict not just *where* an agent looks, but *why*.

2.2 Vison-Language Reasoning

Recent advancements in VLM and LLM have enabled their application across various domains, including scene understanding [18], mathematical problem solving [19], and embodied agent control [20]. They increasingly rely on Chain-of-Thought prompting [21], which forces models to spell out intermediate reasoning [22, 23]. By inserting an explicit reasoning layer between perception and action, these systems plan more reliably and generalise across tasks [24, 25].

We extend this paradigm to virtual-agent head motion, where every turn reflects the agent’s understanding of its goals and surroundings. Unlike saliency or data-driven methods that predict only *where* agents will look, our framework uses VLM–LLM reasoning to infer *why*.

3 Motivation and Problem Statement

Research on realistic virtual-agent behavior has traditionally focused on *macro-level* phenomena, such as crowd simulations [26, 27, 28] or trajectory prediction [29, 30, 31, 32, 33]. By comparison, *micro-level* actions such as head-orientation remain under-explored, even though subtle head shifts strongly influence perceived plausibility in interactive VR and game settings.

Synthesizing natural head turns is challenging because the motion arises from the integration of scene perception, cognitive evaluation, and decision-making. Rather than explicitly modeling these intricate processes, recent studies typically adopt data-driven approaches or visual-saliency proxies [8, 12]. Although such approaches capture conspicuous cues, their shallow treatment of cognition limits generalizability: agents fail to adapt when salient features conflict with task context or social norms, leading to perceptually implausible behaviour in environments.

To overcome these limitations, we first conduct a user study to reveal the underlying rationale behind human head-rotation decisions. Drawing on these insights, we introduce a VLM/LLM–based framework to simulate this decision-making process, enabling robust, data-agnostic head-motion synthesis across diverse and previously unseen scenarios.

4 User Study

Realistic head motion emerges from an agent’s on-the-fly interpretation of visual context and task demands. To replicate such behaviour, we first require an empirical account of *how* and *why* people rotate their heads while navigating immersive environments. The user study, therefore, records human head trajectories in VR together with participants’ own explanations, furnishing both kinematic patterns and the cognitive rationales that produced them. These data subsequently guide the design and validation of our VLM/LLM–driven decision model.

4.1 Apparatus and Settings

The study involved 20 participants (11 males, 9 females; 24.27 ± 2.60 yrs), and all participants had prior experience with VR. We used an Oculus Quest 2 headset driven by a PC (RTX 3090, AMD Ryzen 7 3800XT), paired with controllers.

Five everyday environments (*bus*, *café*, *crosswalk*, *shopping mall*, and *street*) were used for test environments. To collect diverse data, we introduced two distinct experimental conditions:



Figure 2: Red dashed boxes highlight elements present only in the APC version of each environment: a Santa, a traffic accident, and arguing people. The corresponding MDC scenes omit such distracting events.

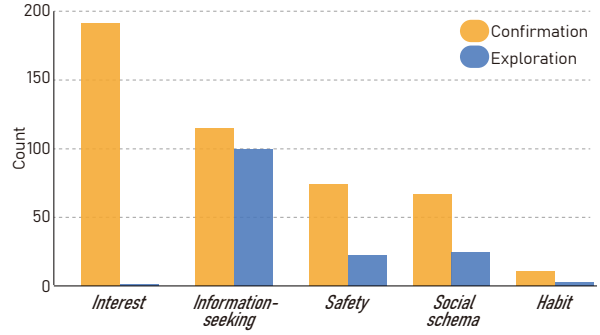


Figure 3: Categorized distribution of participants' self-reported head-movement rationales.

- I. Minimal-Distraction Condition (MDC): A baseline version of each scene in which all objects are static, free of abrupt motion, or high-contrast coloring.
- II. Attention-Provoking Condition (APC): An augmented version of the same layout that embeds distractors: unexpected obstacles, or motion-triggered distractions. Illustrative examples are provided in Figure 2.

4.2 Method and Procedure

A user study was conducted with two experimenters. Upon arrival, each participant provided informed consent and demographic data, then completed a 15-minute orientation (5-minute briefing and *leq*10-minute free navigation in a neutral city scene). Simulator Sickness Questionnaire [34] (SSQ) scores taken before and after the study showed no significant change, and Simulation Task Load Index [35] (SIM-TLX) ratings confirmed low mental workload.

Each participant performed ten 60-second trials covering all combinations of two attentional settings—MDC and APC—and five everyday environments. In each scenario, participants were instructed to complete a scenario-specific goal: *Bus*-find and sit in an empty seat at the back; *Café*-locate and sit at a table by the window; *Crosswalk*-cross safely to the other side; *Shopping Mall*-move from one end of the mall to the opposite side; and *Street*-walk safely to the far end of the street. A 180-second break was available between trials; trial order was randomized to mitigate sequence effects.

We recorded egocentric video, head-orientation quaternions, and sensor data during each scenario. Upon completion of all scenarios, participants reviewed their footage and articulated the underlying motive for every head turn. To facilitate reliable articulation, participants were presented with example prompts such as “*it caught my eye,*” or “*I needed to confirm something.*”

4.3 Derivation of Motivational Drivers

Each head-motion trace was first partitioned into *confirmation turns*, minor intrafoveal shifts used to verify peripheral cues, and *exploration turns*, larger reorientations that probe regions outside the current view. With these classes, movements were further divided into *object-directed* and *information-seeking*. These separations clarified whether a head movement was a check of something already noticed or a deliberate search for new information.

We annotated each trajectory and its 200 accompanying participant explanations. This began with a codebook containing the three motivational factors derived from the attention research—*Safety*, *Interest*, and *Information Seeking* [36, 37, 38]. During iterative review, we observed recurrent behaviours that these labels could not capture, such as surveying the general flow of pedestrians in a shopping mall or tilting the head upward to scan the sky when walking. This led us to define two additional categories, *Social Schema* and *Habit*. The resulting five-factor set constitutes the motivational taxonomy that supports SCORE’s decision model. Figure 3 visualises how often each motivation category appeared in participant explanations across the various scenarios.

5 SCORE Framework

SCORE operates through a two-stage pipeline. Deliberative Perception–Planning Stage (DPS) is the offline planning stage that predicts and schedules the agent’s desired head orientation along the agent’s trajectory. Reactive Execution

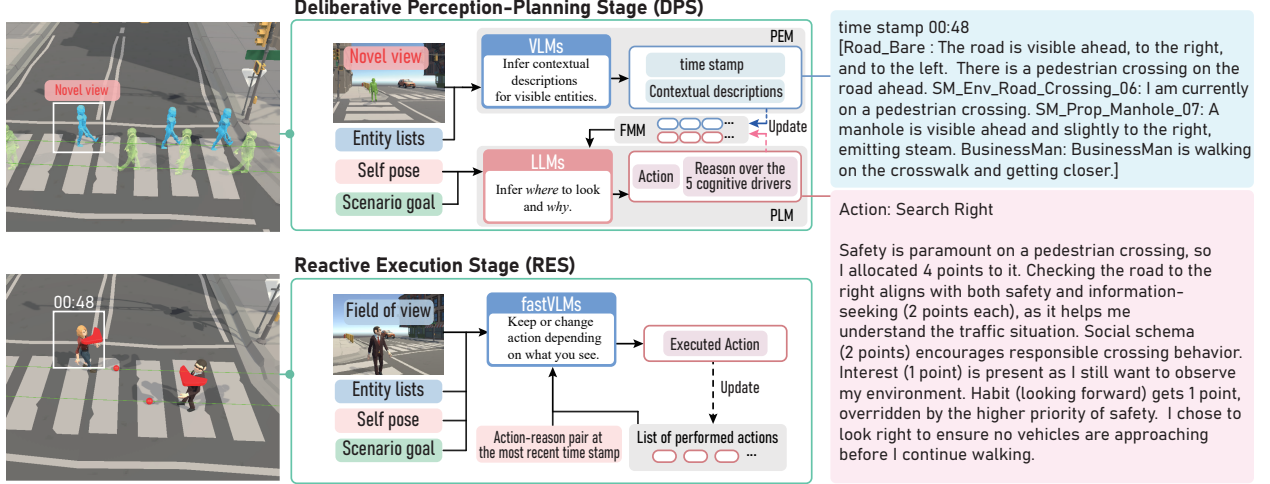


Figure 4: SCORE pipeline. The two-stage architecture combines offline deliberation with near-online refinement. In the DPS, PEM passes each “novel” view, the entity lists, and the scenario goal to a VLM, which generates contextual descriptions stored in FMM. The Planning Module then invokes an LLM that reasons over the five cognitive drivers to select an action–reason pair that schedules the next head orientation. During runtime, RES evaluates a 2-second look-ahead image with a lightweight FastVLM; if the pre-planned action is inconsistent with the live context, it is replaced before execution.

Stage (RES) is the near-online validation stage that refines the pre-planned desired head orientation during runtime. The overall pipeline is shown in Figure 4; implementation details appear in the supplementary.

5.1 Deliberative Perception–Planning Stage (DPS)

DPS runs once for an entire trajectory. At every 0.2s, it submits the agent’s current field of view (FOV) to the Perception Module (PEM). To avoid redundant processing, PEM compares the incoming view image with the most recent “novel” view and flags it as novel only if the Structural Similarity Index Measure (SSIM) [39] between them is below 60 [40]. For each novel view, a forward ray-tracing pass enumerates visible objects and agents. The novel view image, the resulting entity lists, and the scenario goal are then passed to the VLM, which produces contextual descriptions for every entity. These lists and descriptions, stamped with the capture time, are stored in the Foundational Memory Module (FMM).

Afterward, the Planning Module (PLM) invokes an LLM to infer an action–reason pair: the action specifies the target head orientation, and the reason encodes the cognitive motivation. The LLM receives three sources of information: 1) the scenario goal, 2) the agent’s self-pose, and 3) the current FMM contents. Drawing on these, the LLM performs reasoning over the five empirically derived cognitive drivers- *Interest*, *Information Seeking*, *Safety*, *Social Schema*, and *Habit*- to infer an action-reason pair. The pair is appended to the FMM, enabling subsequent decisions to respect behavioral consistency.

DPS simulates the head turn toward the target at $36^\circ/sec$ [41]. During the turn, PEM is paused. Once the target pose is achieved, the agent holds its head for 1-2 seconds $\sim N(1.5, 0.25^2)$. The head then returns to the walking direction, mimicking the human tendency to realign the head after a temporal goal (e.g., threat assessment or curiosity) has been met. PEM resumes after the first half of the head’s hold period, ready to identify the next novel view.

Each FMM entry contains the time stamp, the current object and agent lists, and the associated action–reason pair. To maintain robust performance over long horizons, the FMM retains at most twenty entries: ten are the most recent, and the remainder are those deemed most relevant to the scenario goal according to an LLM-based relevance *SCORE*, following recent agent-memory strategies [42].

All hyperparameters—capture frequency, novelty threshold, and memory size—were tuned empirically to produce plausible motions across the ten test scenarios introduced in the user study.

Table 1: DTW comparison between *IntraHuman*, *Track*, and *SCORE* in single-agent settings across five scenarios under MDC and APC conditions. Lower DTW scores indicate closer alignment with human motion data. The best-performing scores are highlighted in bold. The reported \pm values denote 95% confidence intervals.

Scenario	Method	DTW \downarrow	
		MDC	APC
<i>Bus</i>	<i>IntraHuman</i>	0.2845 \pm .0259	0.3289 \pm .0294
	<i>Track</i>	0.4733 \pm .0233	0.4518 \pm .0186
	<i>SCORE</i> (Ours)	0.4591 \pm .0243	0.4029 \pm .0249
<i>Café</i>	<i>IntraHuman</i>	0.3195 \pm .0246	0.3338 \pm .0261
	<i>Track</i>	0.6367 \pm .0200	0.6550 \pm .0307
	<i>SCORE</i> (Ours)	0.4234 \pm .0251	0.5072 \pm .0283
<i>Crossing</i>	<i>IntraHuman</i>	0.1709 \pm .0174	0.1919 \pm .0225
	<i>Track</i>	0.5611 \pm .0213	0.6504 \pm .0223
	<i>SCORE</i> (Ours)	0.2760 \pm .0191	0.4662 \pm .0241
<i>Mall</i>	<i>IntraHuman</i>	0.5051 \pm .0202	0.2819 \pm .0296
	<i>Track</i>	0.8337 \pm .0355	0.8284 \pm .0183
	<i>SCORE</i> (Ours)	0.5405 \pm .0299	0.4569 \pm .0303
<i>Street</i>	<i>IntraHuman</i>	0.2491 \pm .0205	0.2984 \pm .0248
	<i>Track</i>	0.5999 \pm .0340	0.5912 \pm .0335
	<i>SCORE</i> (Ours)	0.4705 \pm .0298	0.3778 \pm .0397

5.2 Reactive Execution Stage (RES)

RES operates continuously during the simulation. Every 0.2s, it assembles the agent’s current FOV, self-pose, entity list, the scenario goal, the most recent action-reason pair, and the list of actions that actually been performed, and submits this bundle to a lightweight FastVLM. FastVLM determines whether the pre-planned pose remains valid or should be revised. Executed action is logged via the manage schema used in FMM for ensuring dynamic adaptability.

Because FastVLM still requires inference time, RES queries it against a view predicted two seconds ahead of the display frame. This look-ahead window, much shorter than the full VLM–LLM pass yet sufficient for FastVLM, lets *SCORE* operate in a semi-reactive mode that balances latency with scene dynamics. Note that the average inference latencies are 3.50 ± 0.64 (VLM), 7.10 ± 1.22 (LLM), and 1.49 ± 0.41 (FastVLM).

6 Evaluation

In our evaluation, we use Gemini 1.5 Pro as the VLM and LLM for DPS, and Gemini 1.5 Flash [43] as the FastVLM for RES. To assess *SCORE*’s ability to replicate human-like head-motion patterns, we benchmark it against the saliency-driven baseline *Track* [8] and the user-generated motion data collected in the user study (hereafter, *Human*). Similar to prior work that classifies nods and shakes from orientation traces [44, 45], we employ Dynamic Time Warping (DTW) [46] to compare each simulated quaternion sequence with its human counterpart. DTW is well suited to this task: it aligns two time series sample-by-sample while accommodating local speed variations, yielding an interpretable measure of how closely a generated trajectory follows the spatial path taken by real users [47, 48].

6.1 Single-Agent Benchmark

6.1.1 Method

We evaluated *SCORE* on the five distinct virtual scenarios—*Bus*, *Café*, *Crossing*, *Mall*, and *Street*—under both MDC and APC conditions, as used in the user study. For each scenario–condition pair, we generated five head-motion trials with *SCORE* and with *Track*, using the same agent body trajectories that were recorded from the user study and replaying them at a constant walking speed of $1.3m/s$ [49]. All hyperparameters and VLM/LLM prompts were held fixed across scenarios, ensuring a fair comparison.

Table 2: DTW comparison between *Track*, and *SCORE* in multi-agent settings. The best-performing scores are highlighted in bold. The reported \pm values denote 95% confidence intervals.

Scenario	Method	DTW \downarrow
<i>Zara01</i>	<i>Track</i>	0.5632 \pm .0255
	<i>SCORE</i> (Ours)	0.3616 \pm .1015
<i>Zara02</i>	<i>Track</i>	0.4325 \pm .0231
	<i>SCORE</i> (Ours)	0.2657 \pm .0832
<i>students003</i>	<i>Track</i>	0.5621 \pm .0311
	<i>SCORE</i> (Ours)	0.4471 \pm .0956

Head orientation was represented by unit quaternions. The instantaneous angular error between two orientations q_1 and q_2 was computed as

$$d(q_1, q_2) = 2 \cdot \arccos(|\text{dot}(q_1, q_2)|), \quad (1)$$

where $\text{dot}(q_1, q_2)$ denotes the dot product of the quaternions. This instantaneous error served as the local cost function for DTW. DTW then temporally warped one trajectory with respect to the other to identify the alignment that minimizes the accumulated angular error, compensating for local speed differences between the human and simulated motions. The resulting cost was normalised by the mean sequence length to yield a length-invariant similarity score.

Note that *Track* was designed for 360-degree video, predicting salient gaze over a 360° equirectangular image. Applied to first-person navigation with a narrow task-driven FOV, this global-saliency bias is disadvantageous. For a fair comparison, we supply *Track* with only the agent-centred FOV image, and our internal tests confirm that this restriction does not impair its accuracy.

6.1.2 Results

Table 1 provides the normalized DTW scores for both the *Track* and *SCORE*, with lower values denoting closer similarity to the *Human* head-rotation. To provide an upper bound performance, we compute *IntraHuman* baseline. The *Human* is randomly partitioned into two non-overlapping subsets of equal size, and DTW is evaluated between them. Repeating this split ten times and averaging the results yields an empirical lower bound that no model can surpass.

In every scenario, *SCORE* outperforms the saliency baseline *Track*, confirming that first-person context combined with language-based reasoning yields more human-like trajectories.

The advantage is most pronounced in the *Mall* and *Crosswalk*, where rapid scene changes and the presence of multiple objects. *SCORE* also excels in the *Bus-APC* condition: it consistently attends to a Santa Claus passenger who captured participants’ attention, showing that its cognitive layer can infer the social salience of atypical objects.

Across all five environments, *SCORE* maintains low DTW error, demonstrating robust generalization to dynamic layouts, multiple attractors, and culturally nuanced cues. These results emphasize the value of integrating vision–language reasoning into head-motion synthesis for realistic, context-aware virtual agents.

6.2 Multi-Agent Benchmark

6.2.1 Method

To evaluate *SCORE*’s generalizability in multi-agent scenarios, we conducted an additional experiment on the UCY crowd dataset [50], which provides frame-level positions, head orientations, and corresponding video footage. We reproduced three scenes (*zara01*, *zara02*, and *students003*) in our simulator by replicating the recorded agent configurations and environmental layout. The model then generated head-motion trajectories under these conditions, and similarity to the ground-truth orientations was quantified with the DTW metric.

6.2.2 Results

SCORE consistently outperforms the *Track* across all scenes, confirming that its performance scales reliably to multi-agent settings. Qualitatively, the generated head rotations also align closely with human intuition. In *zara01*, the *SCORE* agents spontaneously attend to a shop mannequin, mirroring shoppers’ tendency to glance at salient storefront displays. In *zara02*, the agents shift their head to the new walking direction before turning, much as real pedestrians scan the path ahead when changing course. In *students003*, the agents detect newcomers entering from multiple directions and

Table 3: Responsiveness benchmark with unseen distractors. Any improvement of *MDC-APC* over *MDC-MDC* reflects RES’s ability to detect and adapt to novel stimuli not available at planning time.

Scenario	DTW ↓		
	<i>MDC-MDC</i>	<i>MDC-APC</i>	<i>APC-APC</i>
<i>Bus</i>	0.4330±.0916	0.4182±.0652	0.4029±.0249
<i>Café</i>	0.5505±.1495	0.5255±.0877	0.5072±.0283
<i>Crossing</i>	0.4961±.0723	0.4832±.0555	0.4662±.0241
<i>Mall</i>	0.4909±.0728	0.4724±.0598	0.4569±.0303
<i>Street</i>	0.4875±.0642	0.4322±.0601	0.3778±.0397



Figure 5: Visualization of action and reasoning result when *Interest* is removed from Motivational Drivers.

distribute attention accordingly, reproducing the adaptive scanning seen in crowded situations. Visual examples are provided Figure 6.

6.3 Responsiveness to Unseen Distractors

To evaluate the responsiveness enabled by SCORE’s semi-online RES, we compare model-generated head trajectories under three conditions against *Human* recorded in the APC, using DTW as the similarity metric. The three experimental conditions are defined as follows:

- *MDC-MDC*: Both DPS and RES are run in the MDC. As the model is never exposed to the added distractors present in the APC, this condition serves as a lower bound on performance.
- *MDC-APC*: DPS is executed in the MDC, while RES runs in the APC. Any improvement over *MDC-MDC* reflects RES’s ability to detect and adapt to novel stimuli not available at planning time.
- *APC-APC*: Both DPS and RES run in the APC, giving the model full access to distractors. This represents an upper bound on performance.

Results are reported in Table 3. Notably, *DPS-APC* yields an improvement over *DPS-DPS*, indicating that semi-online validation not only mitigates hallucinations but also enhances responsiveness to scene changes introduced at runtime. Qualitative footage in the supplementary video further illustrates timely reactions to suddenly appearing events, such as an unexpected Santa Claus crossing the field of view.

6.4 Ablation Study

We performed an ablation study to isolate the contribution of *SCORE*’s core components. First, we removed the five symbolic cognitive drivers from the prompts to test whether explicit motivational drivers improve plausibility. All five drivers were removed from the prompt inputs (*w/o all Motivational Drivers*). Furthermore, each driver was selectively excluded while keeping the others intact (*w/o Interest driver*, *w/o Information Seeking driver*, *w/o Safety driver*, *w/o Social Schema driver*, or *w/o Habit driver*). Second, we disabled the LLM and allowed the VLM to choose head poses directly (*w/o LLM*) to evaluate the benefit of a dedicated planning stage. Third, we replaced the deliberative–reactive pipeline with a purely deliberative pass (*w/o RES*) to determine whether the lightweight validation step truly mitigates hallucinations.

We conducted ablation studies in both single- and multi-agent scenarios, with different emphases in terms of motivational drivers. In the single-agent setting, we performed both full ablations. In the multi-agent setting, we limited ablations to the complete removal of all drivers, omitting individual factor tests. This decision was based on two factors: the single-agent results already demonstrate that partial ablations fall between the full model and no-driver baseline, and repeating this in the multi-agent case would add redundancy without yielding new insights.

Results are summarized in Table 4 (single-agent) and Table 5 (multi-agent). Removing cognitive drivers increases DTW error in all scenes, confirming that explicit driver modelling is essential for human-like reasoning. Eliminating the

Table 4: Ablation study of *SCORE* in single-agent settings across five scenarios under MDC and APC conditions.

Scenario	Method	DTW ↓	
		MDC	APC
Bus	<i>SCORE</i>	0.4591 ±.0243	0.4029 ±.0249
	w/o all Motivational Drivers	0.4868±.0299	0.5770±.0293
	w/o Interest driver	0.4622±.0225	0.4571±.0392
	w/o Information-seeking driver	0.4621±.0217	0.4771±.0391
	w/o Safety driver	0.4713±.0267	0.4176±.0261
	w/o Social Schema driver	0.4515±.0315	0.4871±.0297
	w/o Habit driver	0.4719±.0210	0.4470±.0210
	w/o LLM	0.4681±.0289	0.4864±.0363
	w/o RES	0.5594±.0251	0.4202±.0283
Café	<i>SCORE</i>	0.4234 ±.0251	0.5072 ±.0283
	w/o all Motivational Drivers	0.6024±.0330	0.5625±.0318
	w/o Interest driver	0.4521±.0255	0.5141±.0391
	w/o Information-seeking driver	0.4736±.0267	0.5570±.0333
	w/o Safety driver	0.4701±.0259	0.5166±.0290
	w/o Social Schema driver	0.4417±.0227	0.5270±.0298
	w/o Habit driver	0.4320±.0260	0.5161±.0290
	w/o LLM	0.4726±.0309	0.5303±.0417
	w/o RES	0.6517±.0251	0.5798±.0283
Crossing	<i>SCORE</i>	0.2760 ±.0191	0.4662 ±.0241
	w/o all Motivational Drivers	0.5976±.0839	0.5559±.0249
	w/o Interest driver	0.3321±.0226	0.4772±.0291
	w/o Information-seeking driver	0.3021±.0227	0.4871±.0263
	w/o Safety driver	0.4700±.0249	0.5536±.0235
	w/o Social Schema driver	0.3147±.0515	0.4899±.0217
	w/o Habit driver	0.2819±.0220	0.4771±.0255
	w/o LLM	0.3793±.0268	0.5955±.0256
	w/o RES	0.5601±.0251	0.4953±.0283
Mall	<i>SCORE</i>	0.5405 ±.0299	0.4569 ±.0303
	w/o all Motivational Drivers	0.5820±.0433	0.6434±.0276
	w/o Interest driver	0.5721±.0234	0.6570±.0381
	w/o Information-seeking driver	0.5551±.0251	0.4802±.0280
	w/o Safety driver	0.5601±.0355	0.4613±.0333
	w/o Social Schema driver	0.5721±.0321	0.5002±.0265
	w/o Habit driver	0.5723±.0251	0.4901±.0223
	w/o LLM	0.5848±.0168	0.5559±.0159
	w/o RES	0.5081±.0251	0.4542±.0283
Street	<i>SCORE</i>	0.4705 ±.0298	0.3778 ±.0397
	w/o all Motivational Drivers	0.4754±.0251	0.5409±.0300
	w/o Interest driver	0.4741±.0224	0.4999±.0495
	w/o Information-seeking driver	0.4722±.0315	0.4752±.0351
	w/o Safety driver	0.4713±.0260	0.4352±.0200
	w/o Social Schema driver	0.4777±.0210	0.4912±.0390
	w/o Habit driver	0.4773±.0221	0.4510±.0422
	w/o LLM	0.4775±.0393	0.3853±.0486
	w/o RES	0.5167±.0251	0.4150±.0283

LLM and delegating planning entirely to the VLM degrades performance, indicating that a dedicated reasoning stage is essential for producing coherent head trajectories. Finally, omitting the RES amplifies hallucination-induced errors and yields poor scores, demonstrating that FastVLM validation is critical for robust, believable motion. The same trends hold when many agents operate simultaneously, indicating that each component scales effectively to group scenarios.

We additionally visualized how the design of the five factors in our Motivational Drivers impacts the model’s reasoning. As shown in Figure 5, when the *Interest* factor is removed, the agent does not look at Santa even though it is interesting and atypical in the bus. The analysis of other factors can be found in Figure 7.

Table 5: Ablation study of *SCORE* in multi-agent settings across three scenes.

Scenario	Method	DTW ↓
Zara01	<i>SCORE</i>	0.3616 ^{±.1015}
	<i>w/o all Motivational Drivers</i>	0.4721 ^{±.0929}
	<i>w/o LLM</i>	0.4711 ^{±.0939}
	<i>w/o RES</i>	0.5193 ^{±.0840}
Zara02	<i>SCORE</i>	0.2657 ^{±.0832}
	<i>w/o all Motivational Drivers</i>	0.3021 ^{±.0730}
	<i>w/o LLM</i>	0.3125 ^{±.0719}
	<i>w/o RES</i>	0.4116 ^{±.0651}
student003	<i>SCORE</i>	0.4471 ^{±.0956}
	<i>w/o all Motivational Drivers</i>	0.5071 ^{±.0881}
	<i>w/o LLM</i>	0.6192 ^{±.0718}
	<i>w/o RES</i>	0.6102 ^{±.0652}

7 Conclusion

This paper presents *SCORE*, a language-guided framework that couples vision-language perception with language-based reasoning to synthesize human-like head motion. Built on a controlled VR user study, *SCORE* embeds five empirically derived cognitive drivers—*Interest*, *Information-seeking*, *Safety*, *Social schema*, and *Habit*—into a two-stage pipeline. An offline deliberative stage generates a time-stamped head-orientation plan, and an online reactive stage verifies each pose with a lightweight FastVLM, suppressing hallucinations and adapting to late scene changes. Across single- and multi-agent settings, this design more closely replicates human trajectories than the saliency baseline Track, underscoring the value of language-guided cognition for context-aware gaze control.

Three limitations suggest directions for future work. First, augmenting perception with spatial audio and haptic streams would allow agents to respond to non-visual cues such as approaching footsteps or vibration alerts. Second, integrating *SCORE* with a model-predictive navigation controller could unify locomotion and gaze, yielding fully coordinated whole-body behaviour in constrained or collaborative tasks. Third, distilling the LLM into a task-specific lightweight model and caching frequently used predicate patterns in memory may cut inference latency while preserving reasoning depth. Pursuing these extensions could extend *SCORE* to large-scale social VR, robot telepresence, and other applications that demand believable, responsive head motion.

References

- [1] Alon Lerner, Yiorgos Chrysanthou, Ariel Shamir, and Daniel Cohen-Or. Context-dependent crowd evaluation. In *Computer Graphics Forum*, volume 29, pages 2197–2206. Wiley Online Library, 2010.
- [2] Travis Steel, Dane Kuiper, and RZ Wenkstern. Context-aware virtual agents in open environments. In *2010 Sixth International Conference on Autonomic and Autonomous Systems*, pages 90–96. IEEE, 2010.
- [3] Sahil Narang, Andrew Best, Tanmay Randhavane, Ari Shapiro, and Dinesh Manocha. Pedvr: Simulating gaze-based interactions between a real user and virtual crowds. In *Proceedings of the 22nd ACM conference on virtual reality software and technology*, pages 91–100, 2016.
- [4] Cassidy Curtis, Sigurdur Orn Adalgeirsson, Horia Stefan Ciurdar, Peter McDermott, JD Velásquez, W Bradley Knox, Alonso Martinez, Dei Gaztelumendi, Norberto Adrian Goussies, Tianyu Liu, et al. Toward believable acting for autonomous animated characters. In *Proceedings of the 15th ACM SIGGRAPH Conference on Motion, Interaction and Games*, pages 1–15, 2022.
- [5] Yanyu Xu, Yanbing Dong, Junru Wu, Zhengzhong Sun, Zhiru Shi, Jingyi Yu, and Shenghua Gao. Gaze prediction in dynamic 360 immersive videos. In *proceedings of the IEEE Conference on Computer Vision and Pattern Recognition*, pages 5333–5342, 2018.
- [6] Yucheng Zhu, Guangtao Zhai, Xionghuo Min, and Jiantao Zhou. Learning a deep agent to predict head movement in 360-degree images. *ACM Transactions on Multimedia Computing, Communications, and Applications (TOMM)*, 16(4):1–23, 2020.

- [7] Li Yang, Mai Xu, Yichen Guo, Xin Deng, Fangyuan Gao, and Zhenyu Guan. Hierarchical bayesian lstm for head trajectory prediction on omnidirectional images. *IEEE Transactions on Pattern Analysis and Machine Intelligence*, 44(11):7563–7580, 2021.
- [8] MFR Rondon, L Sassatelli, R Aparicio-Pardo, and F Precioso. Track: A new method from a re-examination of deep architectures for head motion prediction in 360° videos. *IEEE Transactions on Pattern Analysis and Machine Intelligence*, 44(9):5681–5699, 2022.
- [9] Rainer Stiefelhagen, Jie Yang, and Alex Waibel. Modeling focus of attention for meeting indexing based on multiple cues. *IEEE Transactions on Neural Networks*, 13(4):928–938, 2002.
- [10] Maria Danninger, Roel Vertegaal, Daniel P Siewiorek, and Aadil Mamuji. Using social geometry to manage interruptions and co-worker attention in office environments. In *Proceedings of Graphics Interface 2005*, pages 211–218. Citeseer, 2005.
- [11] Sileye O Ba and Jean-Marc Odobez. Recognizing visual focus of attention from head pose in natural meetings. *IEEE Transactions on Systems, Man, and Cybernetics, Part B (Cybernetics)*, 39(1):16–33, 2008.
- [12] Anh Nguyen, Zhisheng Yan, and Klara Nahrstedt. Your attention is unique: Detecting 360-degree video saliency in head-mounted display for head movement prediction. In *Proceedings of the 26th ACM international conference on Multimedia*, pages 1190–1198, 2018.
- [13] Ching-Ling Fan, Jean Lee, Wen-Chih Lo, Chun-Ying Huang, Kuan-Ta Chen, and Cheng-Hsin Hsu. Fixation prediction for 360 video streaming in head-mounted virtual reality. In *Proceedings of the 27th workshop on network and operating systems support for digital audio and video*, pages 67–72, 2017.
- [14] A Deniz Aladagli, Erhan Ekmekcioglu, Dmitri Jarnikov, and Ahmet Kondo. Predicting head trajectories in 360 virtual reality videos. In *2017 International Conference on 3D Immersion (IC3D)*, pages 1–6. IEEE, 2017.
- [15] Feng Qian, Lusheng Ji, Bo Han, and Vijay Gopalakrishnan. Optimizing 360 video delivery over cellular networks. In *Proceedings of the 5th Workshop on All Things Cellular: Operations, Applications and Challenges*, pages 1–6, 2016.
- [16] Fanyi Duanmu, Eymen Kurdoglu, S Amir Hosseini, Yong Liu, and Yao Wang. Prioritized buffer control in two-tier 360 video streaming. In *Proceedings of the Workshop on Virtual Reality and Augmented Reality Network*, pages 13–18, 2017.
- [17] Ashesh Jain, Amir R Zamir, Silvio Savarese, and Ashutosh Saxena. Structural-rnn: Deep learning on spatio-temporal graphs. In *Proceedings of the IEEE conference on computer vision and pattern recognition*, pages 5308–5317, 2016.
- [18] Rao Fu, Jingyu Liu, Xilun Chen, Yixin Nie, and Wenhan Xiong. Scene-llm: Extending language model for 3d visual understanding and reasoning. *arXiv preprint arXiv:2403.11401*, 2024.
- [19] Zhenwen Liang, Tianyu Yang, Jipeng Zhang, and Xiangliang Zhang. Unimath: A foundational and multimodal mathematical reasoner. In *Proceedings of the 2023 Conference on Empirical Methods in Natural Language Processing*, pages 7126–7133, 2023.
- [20] Moo Jin Kim, Karl Pertsch, Siddharth Karamcheti, Ted Xiao, Ashwin Balakrishna, Suraj Nair, Rafael Rafailov, Ethan Foster, Grace Lam, Pannag Sanketi, et al. Openvla: An open-source vision-language-action model. *arXiv preprint arXiv:2406.09246*, 2024.
- [21] Jason Wei, Xuezhi Wang, Dale Schuurmans, Maarten Bosma, Fei Xia, Ed Chi, Quoc V Le, Denny Zhou, et al. Chain-of-thought prompting elicits reasoning in large language models. *Advances in neural information processing systems*, 35:24824–24837, 2022.
- [22] Shunyu Yao, Jeffrey Zhao, Dian Yu, Nan Du, Izhak Shafran, Karthik Narasimhan, and Yuan Cao. React: Synergizing reasoning and acting in language models. In *International Conference on Learning Representations (ICLR)*, 2023.
- [23] Noah Shinn, Federico Cassano, Ashwin Gopinath, Karthik Narasimhan, and Shunyu Yao. Reflexion: Language agents with verbal reinforcement learning. *Advances in Neural Information Processing Systems*, 36:8634–8652, 2023.
- [24] Chan Hee Song, Jiaman Wu, Clayton Washington, Brian M Sadler, Wei-Lun Chao, and Yu Su. Llm-planner: Few-shot grounded planning for embodied agents with large language models. In *Proceedings of the IEEE/CVF international conference on computer vision*, pages 2998–3009, 2023.
- [25] Zhengyuan Yang, Linjie Li, Jianfeng Wang, Kevin Lin, Ehsan Azarnasab, Faisal Ahmed, Zicheng Liu, Ce Liu, Michael Zeng, and Lijuan Wang. Mm-react: Prompting chatgpt for multimodal reasoning and action. *arXiv preprint arXiv:2303.11381*, 2023.

- [26] Andreas Panayiotou, Theodoros Kyriakou, Marilena Lemonari, Yiorgos Chrysanthou, and Panayiotis Charalambous. Ccp: Configurable crowd profiles. In *ACM SIGGRAPH 2022 conference proceedings*, pages 1–10, 2022.
- [27] Panayiotis Charalambous, Julien Pette, Vassilis Vassiliades, Yiorgos Chrysanthou, and Nuria Pelechano. Greilcrowds: crowd simulation with deep reinforcement learning and examples. *ACM Transactions on Graphics (TOG)*, 42(4):1–15, 2023.
- [28] Xuebo Ji, Zherong Pan, Xifeng Gao, and Jia Pan. Text-guided synthesis of crowd animation. In *ACM SIGGRAPH 2024 Conference Papers*, pages 1–11, 2024.
- [29] Jiangbei Yue, Dinesh Manocha, and He Wang. Human trajectory prediction via neural social physics. In *European conference on computer vision*, pages 376–394. Springer, 2022.
- [30] Ke Guo, Wenxi Liu, and Jia Pan. End-to-end trajectory distribution prediction based on occupancy grid maps. In *Proceedings of the IEEE/CVF Conference on Computer Vision and Pattern Recognition*, pages 2242–2251, 2022.
- [31] Xiaotong Lin, Tianming Liang, Jianhuang Lai, and Jian-Fang Hu. Progressive pretext task learning for human trajectory prediction. In *European Conference on Computer Vision*, pages 197–214. Springer, 2025.
- [32] Conghao Wong, Beihao Xia, Ziming Hong, Qinmu Peng, Wei Yuan, Qiong Cao, Yibo Yang, and Xinge You. View vertically: A hierarchical network for trajectory prediction via fourier spectrums. In *European Conference on Computer Vision*, pages 682–700. Springer, 2022.
- [33] Karttikeya Mangalam, Yang An, Harshayu Girase, and Jitendra Malik. From goals, waypoints & paths to long term human trajectory forecasting. In *Proceedings of the IEEE/CVF International Conference on Computer Vision*, pages 15233–15242, 2021.
- [34] Robert S Kennedy, Norman E Lane, Kevin S Berbaum, and Michael G Lilienthal. Simulator sickness questionnaire: An enhanced method for quantifying simulator sickness. *The international journal of aviation psychology*, 3(3):203–220, 1993.
- [35] David Harris, Mark Wilson, and Samuel Vine. Development and validation of a simulation workload measure: the simulation task load index (sim-tlx). *Virtual Reality*, 24(4):557–566, 2020.
- [36] Yue Yang, Yee Mun Lee, Ruth Madigan, Albert Solernou, and Natasha Merat. Interpreting pedestrians’ head movements when encountering automated vehicles at a virtual crossroad. *Transportation research part F: traffic psychology and behaviour*, 103:340–352, 2024.
- [37] Harry J Witchel, Carlos P Santos, James K Ackah, Carina EI Westling, and Nachiappan Chockalingam. Non-instrumental movement inhibition (nimi) differentially suppresses head and thigh movements during screenic engagement: dependence on interaction. *Frontiers in Psychology*, 7:157, 2016.
- [38] Ethan S Bromberg-Martin and Ilya E Monosov. Neural circuitry of information seeking. *Current Opinion in Behavioral Sciences*, 35:62–70, 2020.
- [39] Zhou Wang, Alan C Bovik, Hamid R Sheikh, and Eero P Simoncelli. Image quality assessment: from error visibility to structural similarity. *IEEE transactions on image processing*, 13(4):600–612, 2004.
- [40] Sandeep Kumar Yedla, VM Manikandan, and V Panchami. Real-time scene change detection with object detection for automated stock verification. In *2020 5th International Conference on Devices, Circuits and Systems (ICDCS)*, pages 157–161. IEEE, 2020.
- [41] Gerard E Grossman, R John Leigh, Larry A Abel, Douglas J Lanska, and SE Thurston. Frequency and velocity of rotational head perturbations during locomotion. *Experimental brain research*, 70:470–476, 1988.
- [42] SeungWon Seo, SeongRae Noh, Junhyeok Lee, SooBin Lim, Won Hee Lee, and HyeongYeop Kang. Reveca: Adaptive planning and trajectory-based validation in cooperative language agents using information relevance and relative proximity. In *Proceedings of the AAAI Conference on Artificial Intelligence*, volume 39, pages 23295–23303, 2025.
- [43] Gemini Team, Petko Georgiev, Ving Ian Lei, Ryan Burnell, Libin Bai, Anmol Gulati, Garrett Tanzer, Damien Vincent, Zhufeng Pan, Shibo Wang, et al. Gemini 1.5: Unlocking multimodal understanding across millions of tokens of context. *arXiv preprint arXiv:2403.05530*, 2024.
- [44] Adam Switonski, Henryk Josinski, and Konrad Wojciechowski. Dynamic time warping in classification and selection of motion capture data. *Multidimensional Systems and Signal Processing*, 30:1437–1468, 2019.
- [45] Huaizhou Li and Haiyan Hu. Head gesture recognition combining activity detection and dynamic time warping. *Journal of Imaging*, 10(5):123, 2024.
- [46] Hiroaki Sakoe and Seibi Chiba. Dynamic programming algorithm optimization for spoken word recognition. *IEEE transactions on acoustics, speech, and signal processing*, 26(1):43–49, 1978.

- [47] Marco Cuturi and Mathieu Blondel. Soft-dtw: a differentiable loss function for time-series. In *International conference on machine learning*, pages 894–903. PMLR, 2017.
- [48] Hugo Lerogeron, Romain Picot-Clemente, Alain Rakotomamonjy, and Laurent Heutte. Approximating dtw with a convolutional neural network on eeg data. *arXiv preprint arXiv:2301.12873*, 2023.
- [49] Richard W Bohannon. Comfortable and maximum walking speed of adults aged 20—79 years: reference values and determinants. *Age and ageing*, 26(1):15–19, 1997.
- [50] Alon Lerner, Yiorgos Chrysanthou, and Dani Lischinski. Crowds by example. In *Computer graphics forum*, volume 26, pages 655–664. Wiley Online Library, 2007.

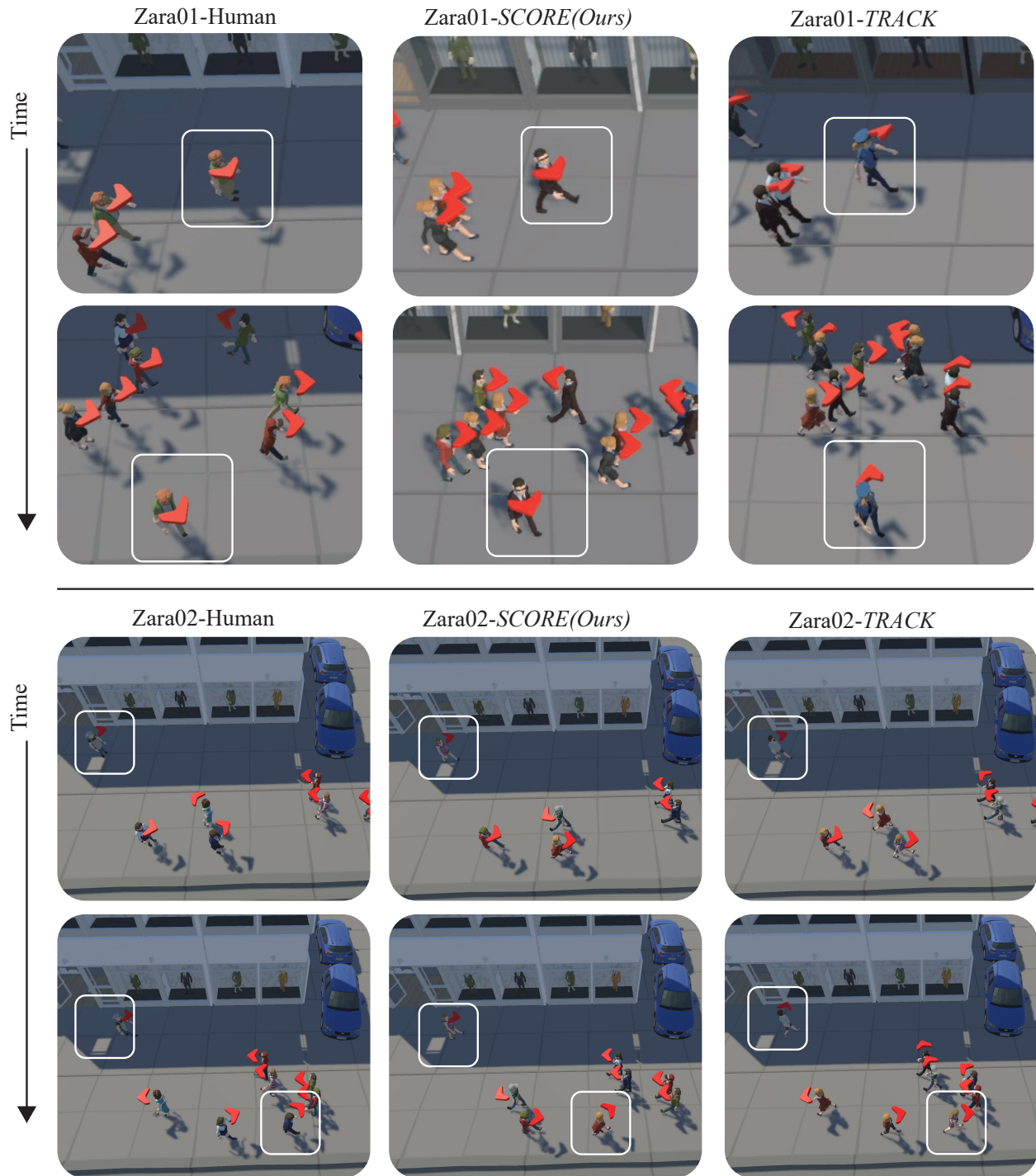


Figure 6: This example illustrates how *SCORE* produces human-like head movements in a multi-agent setting. The highlighted agent attends to the intended walking path, aligning closely with the ground-truth behavior. In contrast, *Track* fixates excessively on static background elements (e.g., storefronts), failing to handle multiple factors (e.g., secure path, understand pedestrian flow) and resulting in implausible head rotations.



Figure 7: Visualization of reasoning and action when *Information-seeking*, *Habit*, *Safety* and *Social schema* are excluded from the motivational drivers.

A Implementation details

All experiments were conducted in a Unity environment running on Windows 10. The project was implemented using Unity version 2022.3.55f1. For the Deliberative Perception–Planning Stage (DPS), we employed Gemini 1.5 Pro, a high-performance Large Language Model (LLM) and Vision Language Model (VLM) developed by Google DeepMind, capable of processing both text and images with high accuracy and strong reasoning capabilities. For the Reactive Execution Stage (RES), we employed Gemini 1.5 Flash, a lightweight variant of the model optimized for low-latency inference [43].

B Single-agent Human dataset details

This supplementary section presents representative samples from our single-agent user study. Each example highlights the object selected by a participant, their corresponding rationale, and a first-person Field-of-View (FoV) image illustrating the interaction. The visualizations are shown in Figure 8, Figure 9, Figure 10, Figure 11, and Figure 12.

These examples demonstrate that participants not only followed their assigned cognitive goals but also engaged in naturalistic attentional shifts and exploratory behaviors. Each FoV visualization includes a randomly assigned participant ID at the top for identification. The primary object(s) of focus within the scene are highlighted in yellow.

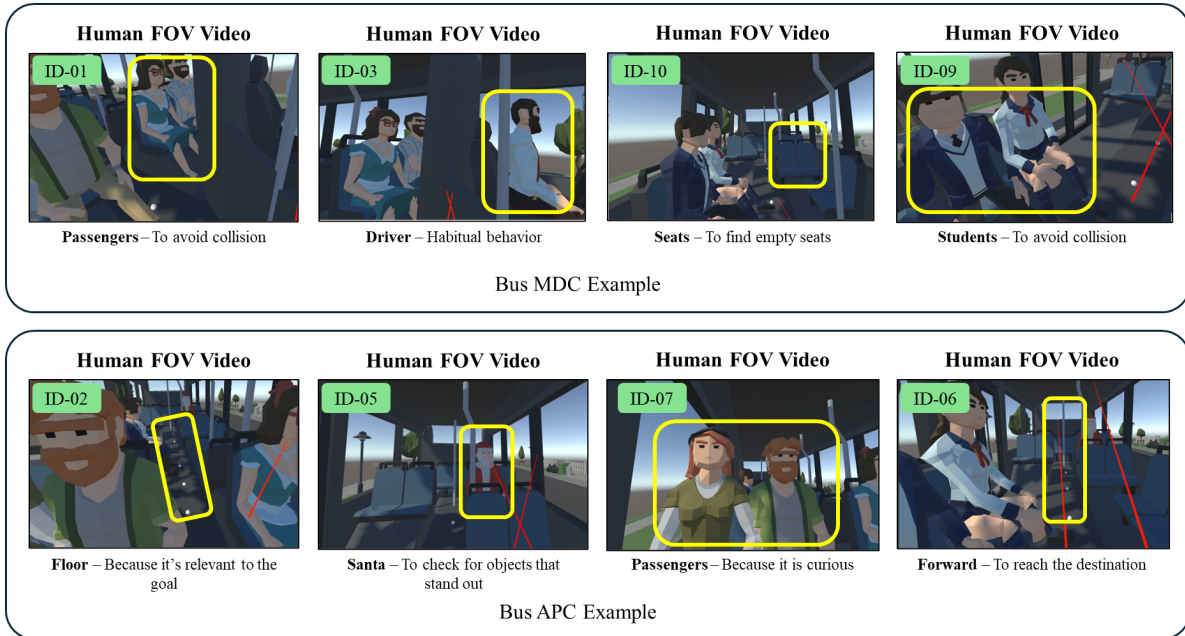


Figure 8: Bus scenario: MDC and APC example. This example demonstrates participant behavior under the cognitive goal of “move to the back.” While complying with the instructed task, participants often fixate on contextually salient or socially relevant entities, such as observing the bus driver or scanning for interesting individuals. The yellow highlights indicate the primary objects of attention within the FoV.

C Single-agent head rotation visualization

To intuitively assess how closely our generated head orientations resemble those of humans in a single-agent scenario, we visualize the 3D head rotations over time by projecting them onto a spherical model. Specifically, we extract corresponding data from the human data collected in the user study and compare them with the head trajectory generated by our model, SCORE, as well as by the *Track*. All time steps of head orientation are plotted as trajectories on a sphere, allowing for clear visual comparison.

Figure 13, Figure 14, Figure 15, Figure 16 and Figure 17 illustrate these visualizations. As shown, the head rotation patterns produced by SCORE demonstrate a strong resemblance to human behavior. This visualization provides compelling qualitative evidence of the alignment between our model’s output and natural human head movements.

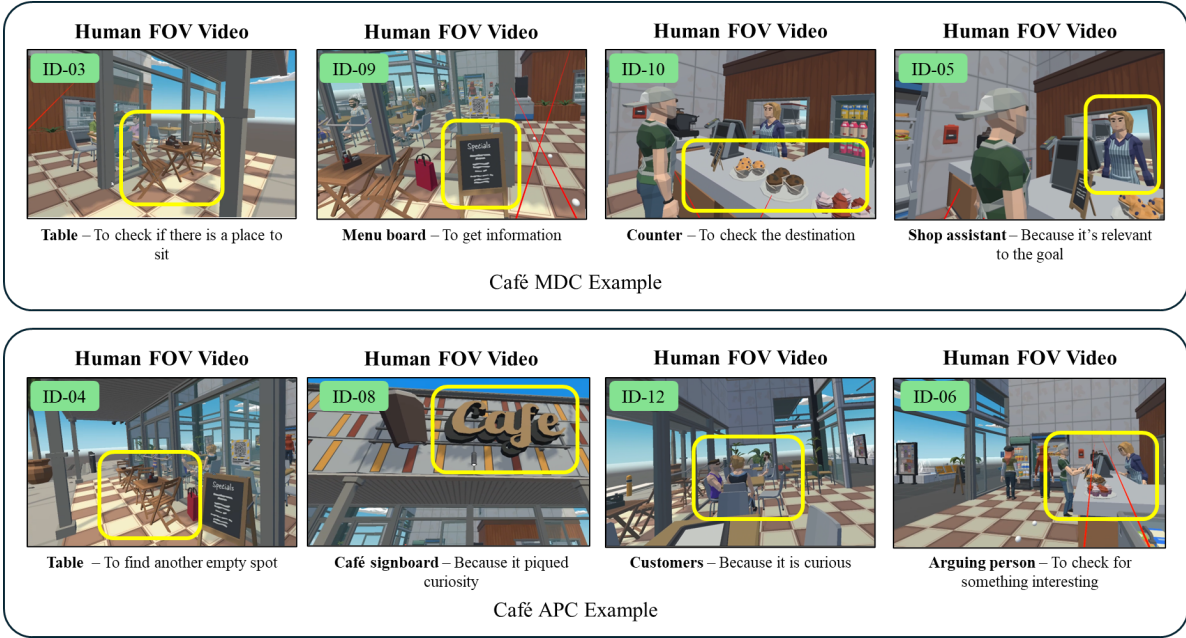


Figure 9: Café scenario: MDC and APC example. This example demonstrates participant behavior under the cognitive goal of “find an empty seat and move toward the counter.” The yellow highlights indicate the primary objects of attention within the FoV.

D Multi-agent dataset details

For our experiments, we utilized the UCY crowd dataset [50], a publicly available collection of annotated video sequences widely used for pedestrian trajectory prediction and crowd behavior research. The UCY dataset provides rich annotations of real-world human motion captured in outdoor university settings, using a static overhead camera to simplify perspective distortions and facilitate accurate tracking. Each sequence contains 2D trajectories of pedestrians, manually annotated at a temporal resolution of 2.5 Hz (i.e., one frame every 0.4 seconds).

We specifically employ three sequences from the dataset: Zara01, Zara02, and Students003. Both Zara01 and Zara02 were recorded in a semi-structured pedestrian area adjacent to a shopping complex. These sequences exhibit relatively sparse pedestrian densities, averaging around 5–6 individuals per frame. The scenes include distinct environmental features such as sidewalks, storefronts, doors, walls, and curbs, which naturally guide pedestrian behavior. These sequences capture a wide variety of naturalistic actions, including individuals pausing to look at shop windows, changing direction mid-path, and interacting with environmental obstacles. Due to their clarity and behavioral diversity, these sequences are particularly valuable for extracting examples of nuanced, individualized motion patterns.

In contrast, the Students003 sequence was recorded during a break period outside a university building and represents a dense crowd scenario, with approximately 40 individuals present per frame on average. The setting captures complex inter-agent interactions, such as collision avoidance, local grouping behavior, and flow pattern emergence, making it ideal for studying high-density crowd dynamics. Together, these three sequences offer a complementary set of crowd conditions, ranging from isolated motion to densely packed social navigation, which serve as the foundation for constructing a robust, example-driven crowd simulation model.

E System prompt Details

Figure 18 illustrates the prompt used in the VLM of the DPS, while Figure 19 shows the corresponding prompt employed in the LLM. Furthermore, Figure 20 presents the prompt designed for the FastVLM model of the RES setting. These prompts were carefully crafted to suit the specific characteristics and tasks of each model, enabling consistent and fair comparisons across different modalities.

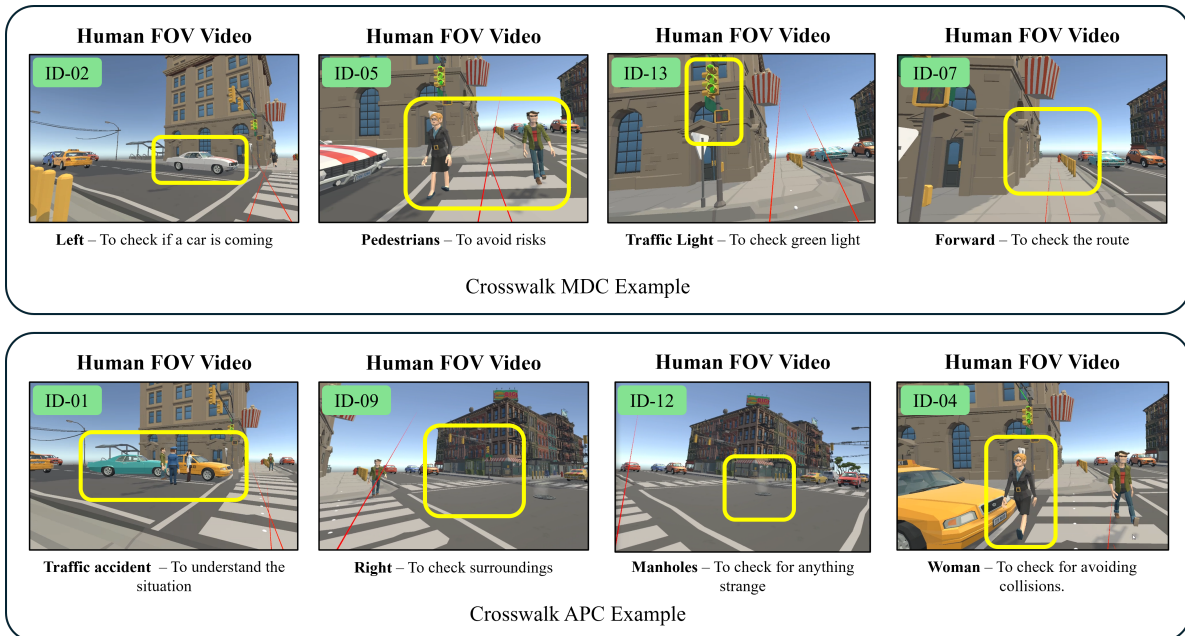


Figure 10: Crosswalk scenario: MDC and APC example. This example demonstrates participant behavior under the cognitive goal of “safely cross the street.” Participants predominantly focus on safety-relevant cues, such as traffic signals or oncoming vehicles, while intermittently scanning for other engaging elements. The yellow highlights indicate the primary objects of attention within the FoV.

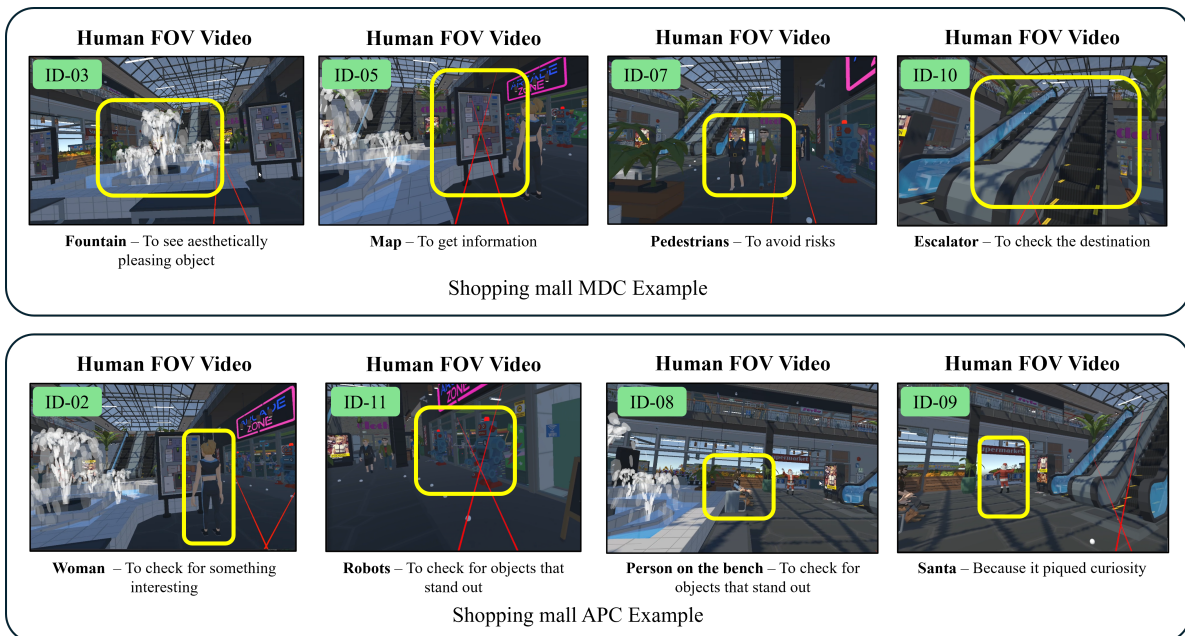


Figure 11: Shopping mall scenario: MDC and APC example. This example demonstrates participant behavior under the cognitive goal of “move toward the escalator.” Despite the visual and semantic complexity of the environment, participants effectively maintained goal-directed behavior while attending to notable objects, such as a map for navigation or visually salient entities. The yellow highlights indicate the primary objects of attention within the FoV.

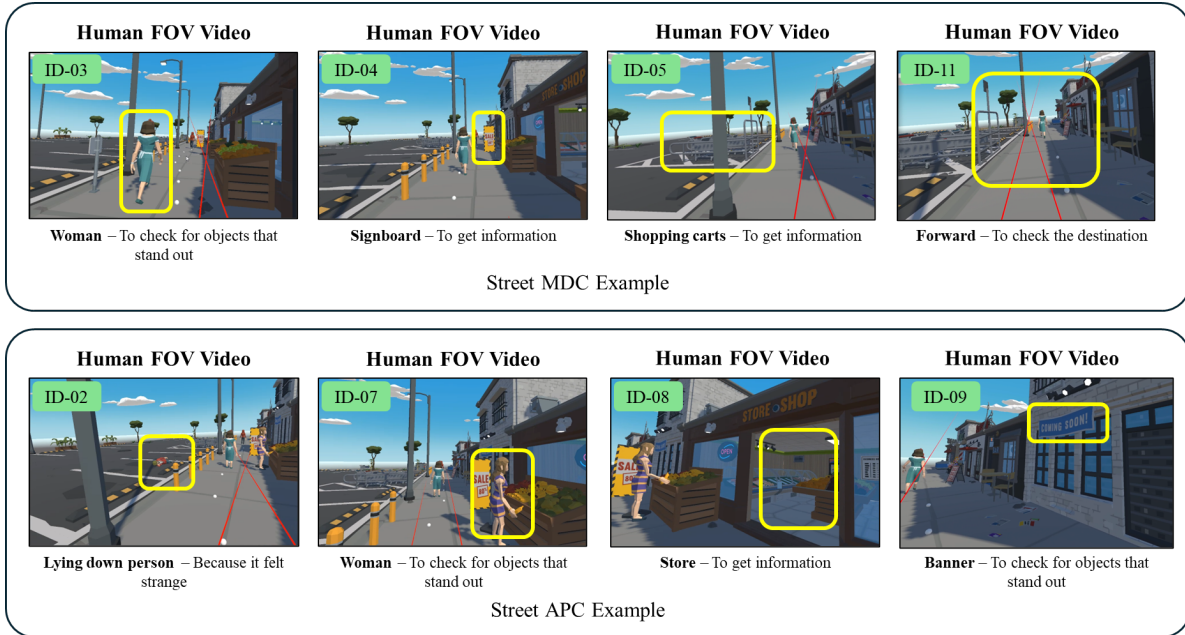


Figure 12: Street scenario: MDC and APC example. This example demonstrates participant behavior under the cognitive goal of “walk safely along the street.” Many participants showed heightened attention toward unexpected or socially salient elements, such as an individual lying on the ground. The yellow highlights indicate the primary objects of attention within the FoV.

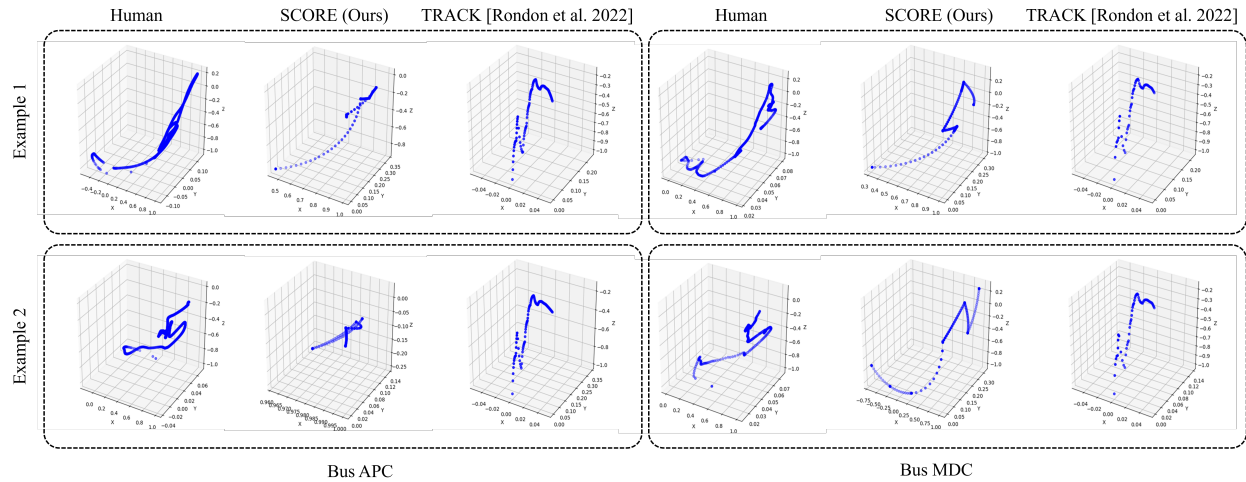


Figure 13: Visualization of head rotation examples in the *Bus* scenario, including both APC and MDC cases. Each plot shows the tracking of the spherical model across all timesteps.

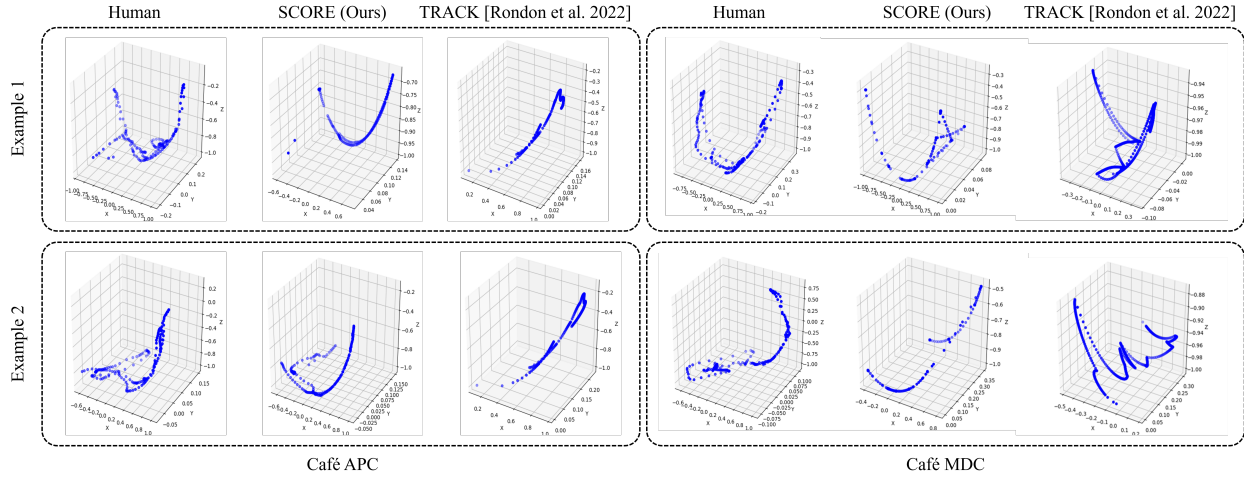


Figure 14: Visualization of head rotation examples in the *Café* scenario.

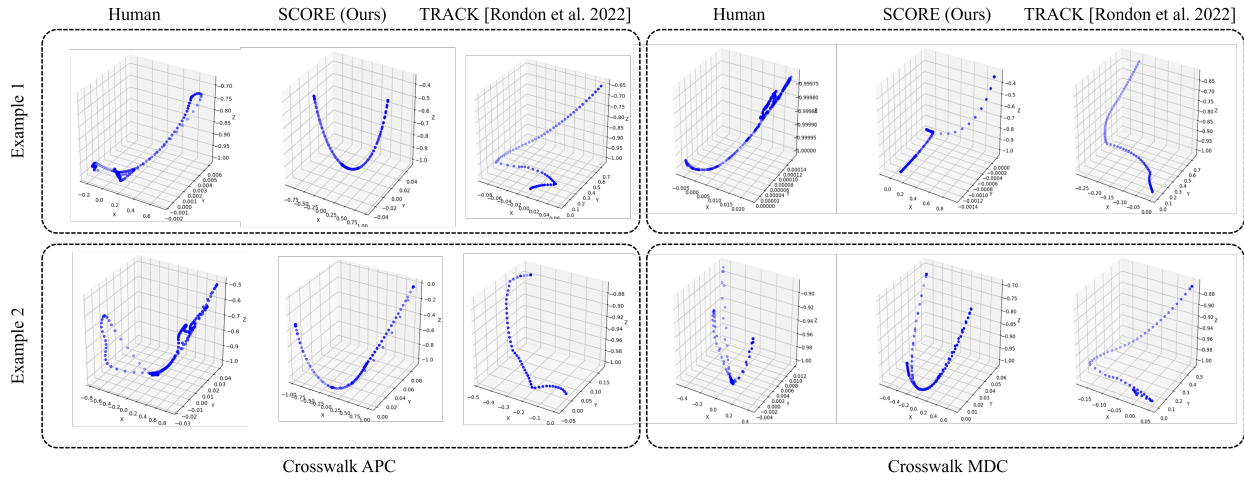


Figure 15: Visualization of head rotation examples in the *Crossing* scenario.

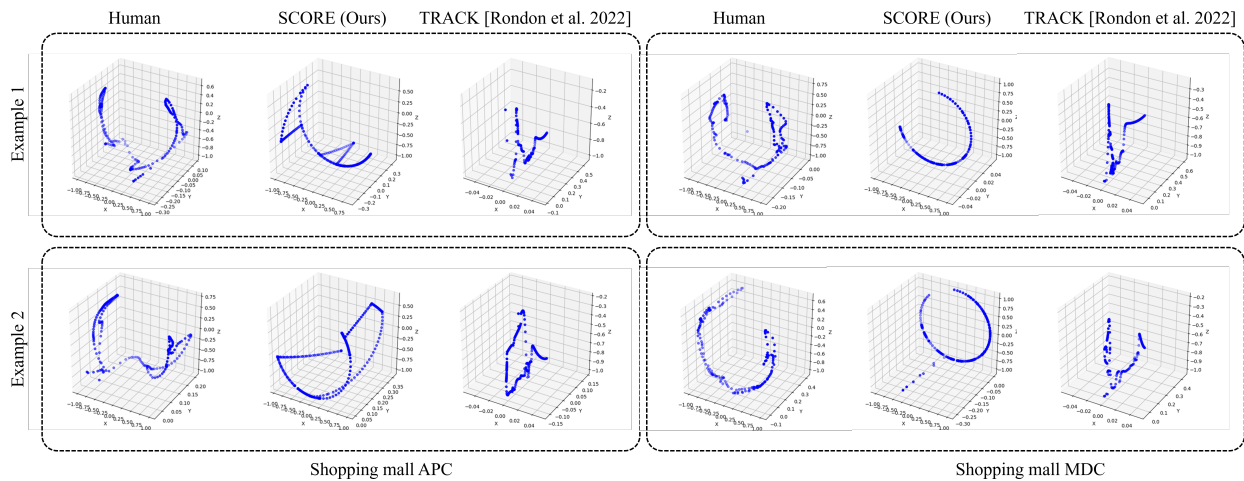


Figure 16: Visualization of head rotation examples in the *Mall* scenario.

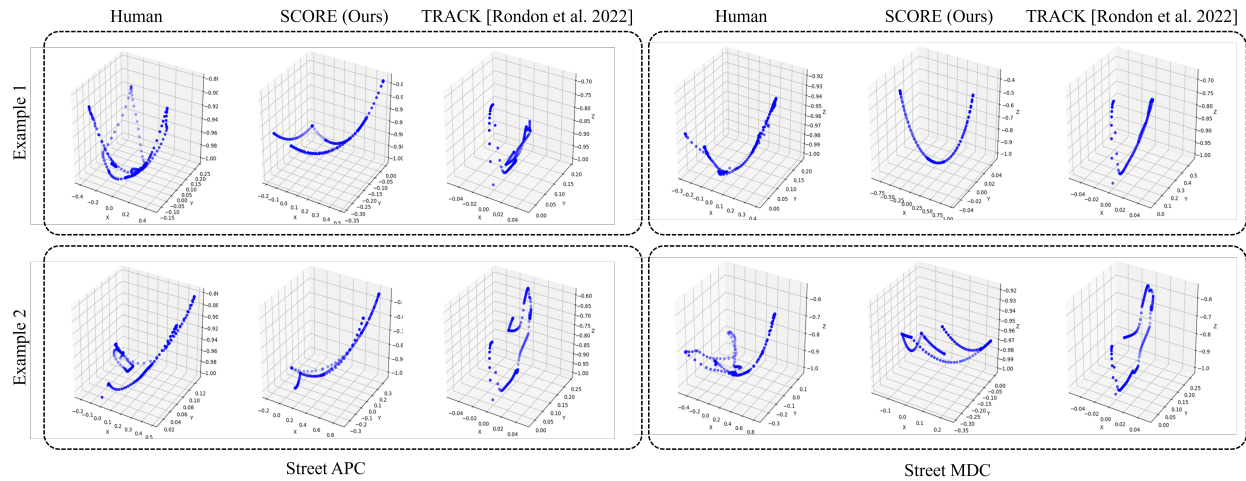


Figure 17: Visualization of head rotation examples in the *Street* scenario.

DPS-VLM Prompt

You are a person navigating through an environment. You understand that vision plays a crucial role in interacting with appropriately with your surroundings-both to discover interesting things and to avoid potential dangers. And be careful-if your neck twists too far, you stop looking human.

Here is the information currently available to you:

- Scenario goal: {cognitive_goal}
- Current Memory: {vlmMemory}
- Entity List: {visibleObjectAgent}

#Stage 1: Memory Update

Your task is to match the given image input with the provided Entity list and generate updated descriptions for each object.

Strategy:

0. Do not add any information about objects that are not in the provided object list. And Do not change the object name in list.
1. Update the memory with information about the top 10 objects from the object list that are most closely related to the Scenario goal.
2. If new information is observed about these objects (e.g., updated position, state, or attributes), incorporate it into the memory.
3. Retain any previously known information that remains valid and is not contradicted by new observations.
4. If an object is relevant to the Cognitive Goal, include that in the memory update.

STRICT NAMING POLICY

You must **never** introduce, reference, or invent any object or entity name that does **not** appear verbatim in the “Entity List” above.

Output Format:

Final Output Format:

---MEMORY---

[Name1 : explain1,

Name2 : explain2,

Name3 : explain3,

...]

Figure 18: The prompt used in the VLM of the DPS.

DPS-LLM Prompt

You are a person navigating through an environment. You understand that vision plays a crucial role in interacting with appropriately with your surroundings-both to discover interesting things and to avoid potential dangers. And be careful-if your neck twists too far, you stop looking human.

You are deciding by 0.2 seconds.

Here is the information currently available to you:

- Cognitive goal: {cognitive_goal}
- Current Memory: {vlmMemory}
- Entity list: {visibleObjectAgent}
- Visual Information Summary: {visualSummary}
- History Decision Actions: {futureActionHistoryLog}
- Current Head Quaternion: ({futureHeadController.futureHead.rotation.x}, {futureHeadController.futureHead.rotation.y}, {futureHeadController.futureHead.rotation.z}, {futureHeadController.futureHead.rotation.w})
- Your head is turned(x: {xDiff}, y: {yDiff}) degrees away from your body.

Decision Making

Instructions:

Step 1: Task Manager

1. **Cognitive Goal Analysis:** Break down the cognitive goal into specific and actionable subtasks.
2. **Subtask Objectives:** Create five subtasks, each focusing on one of the following dimensions:
 - **Safety:** Actions that minimize risk or ensure physical security.
 - **Interest:** Actions that fulfill curiosity or inquisitiveness.
 - **Social Schema:** Actions aligned with social norms.
 - **Information-Seeking:** Actions aimed at acquiring more details or clarifying uncertain aspects of the environment. If the object list is insufficient, consider exploring the environment to gather additional information.
 - **Habit:** Common human routines.

Step 2: Decision and Action

1. **Decision Process:**

- Check whether the cognitive goal can be addressed using any object from the Object List.
- If not, or if exploration would better serve the goal, choose to explore based on the context.
- You are deciding by 0.2 seconds.

2. **Action Types:**

- For known objects: Output must be `""Looking at<object name>""`. Only include object names from the `""Object List""`. And Do not add any explanations or descriptions after the action.
- For exploration: Output must be `""Search <direction>""`, where `direction` \in [forward]. Only one direction can be selected.

Final Constraints:

- You must only select from the `""Object List""` when focusing on an object.
- Include in Explanation why you chose the action

###Final Scoring Instruction

After deciding the action, distribute a total of 10 points across the five subtasks (Safety, Interest, Social Schema, Information-Seeking, Habit) to indicate your focus.

Output Format:

Final Output Format:

---Scores---

[SafetyScore, InterestScore, SocialSchemaScore, InformationSeekingScore, HabitScore]

---Explanation---

[Your explanation here]

---Action---

[Your final action here - either `""Looking at <object name>""`]

Figure 19: The prompt used in the LLM of the DPS.

RES-FastVLM Prompt

You are a person navigating through an environment. You understand that vision plays a crucial role in interacting appropriately with your surroundings-both to discover interesting things and to avoid potential dangers. And be careful-if you twist your neck too far, you stop looking human.

Here is the information currently available to you:

- Entity List: {visibleObjectAgent}
- Scheduled action: {agentData.GetClosestAction(this.transform.position)}
- Executed Action List: {excutedActionList}
- Your head is turned(x: {currentMovement.GetDiffValue().x}, y: {currentMovement.GetDiffValue().y}) degrees away from your body.
- Directions you are moving: {this.transform.forward}

Please decide:

- Have you detected any movement from other agents in the image list that might pose a threat or very interesting?
- If it is true, adjust your head movement. The actions you can take are:
 1. For known agents: Output must be "**Looking at <Agent name>**". Only use names from the "Agent List". Do not add any explanations or descriptions after the action.
 2. If no adjustment is needed: **keep**

Output Format:

---Action---

[Your final action here-either "Looking at <Agent name>" or keep]

Figure 20: The prompt used in the FastVLM of the RES.